ROBUST SENSING AND CONTROL OF WELD POOL SURFACE

Wei Lu, Yu-Ming Zhang, Chuan Zhang, and Bruce L. Walcott

Department of Electrical and Computer Engineering
University of Kentucky, Lexington, KY 40506, USA

Abstract: Gas tungsten arc welding is the primary process for precision joining of metals. To develop a simple yet durable sensing and control system for this process, a novel sensor which requires no additional attachment is proposed to sense the depth of the weld pool surface using a non-transferred arc. To assure its effectiveness and accuracy, a flat surface is periodically established to provide a real-time reference so that the weld pool surface depth can be accurately measured. Because of possible large process variations, an interval model control algorithm with adaptively updated intervals is adopted. Closed-loop experiments showed that the developed control system is capable of achieving quality welds and is robust with respect to different variations.

Keywords: Predictive control; Adaptive control; Uncertainty; Manufacturing processes; Sensor system.

1. INTRODUCTION

Arc welding has become an essential tool for metal joining in modern industries. Among them are two prominent technologies: Plasma Arc Welding (PAW) and Gas Tungsten Arc Welding (GTAW). PAW, basically a modification of GTAW, has higher arc energy density and plasma gas velocity by virtue of the arc plasma being forced through a constricting nozzle (American Welding Society 1990). Hence, PAW can be applied at higher speed and lower current than GTAW for certain applications, resulting in less welding shrinkage and distortion. However, GTAW is still an indispensable tool in precision joining because of its softer arc which is easier to control, especially for the root pass where the weld joint penetration must be assured. Hence, the monitoring and control of weld joint penetration in GTAW is an important issue the welding research community must address and find good solutions for.

Although the state of the weld joint penetration is typically measured by the back-side width of the weld bead, most existing penetration sensing methods use front-side sensors, which can be attached to and move with the welding torch, because it is not convenient to access the back-side in most applications. As a result, the weld joint penetration needs to be estimated from measurements acquired from the front-side. For example, Richardson (Renwick and Richardson,1983) and den Ouden (Anedenroomer and den Ouden, 1998) utilized the weld pool oscillation to estimate the weld joint penetration. Ume and his students (Hopko and Ume, 1999; Bai and Ume, 2004) used ultrasonic signals to calculate/estimate the weld pool depth. Chin and his

students (Fan et al., 2003) developed a point infrared sensing system to monitor the welding process. For vision based methods, Wu and his student (Gao and Wu, 2003) and Chen and his colleagues (2000) used regular CCD cameras to measure the weld pool shape in pulsed arc welding during the base current period, and Zhang (1990) used structured-light method to measure the weld sag right behind the weld pool in order to estimate the weld joint penetration. Though these methods work for certain applications, simple yet effective and robust solutions which can lead to wide industrial applications are still highly desired.

Since weld pool is closely correlated to the penetration, its observation appears a more direct and desirable approach for joint penetration monitoring. However, an optical measurement of the weld pool may not be technically or economically applicable for most applications. Because the welding arc has a close contact with the weld pool, it may be possible to measure the weld pool using the arc as the sensing device without additional attachment. However, the welding arc has only been used in the through-the-arc method (Koseeyaorn and Cook, 1999) for measuring the arc length for arc length control and seam tracking based on the fact that the arc voltage is proportional to the arc length when other parameters, such as welding current, shielding gas flow rate, etc, are fixed. In applications where high precision is critical, the transferring nature of typical welding arcs limits the precision achievable because the trajectories of the electrons are not straight and subject to the effect of the geometry of the electrodes such as the shape of the weld pool surface (Fig. 1(a)). Precise measurement of the depth of the weld pool surface requires the measurement of a straight distance with an idea arc behavior, shown in Fig. 1(b), which is not subject to the effect of the weld pool surface shape.

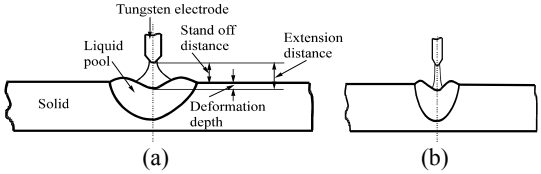

Fig. 1. Arc Behavior and Weld Pool Surface.
(a) Influence of Weld Pool Profile on Arc Behavior.
(b) Ideal Behavior.

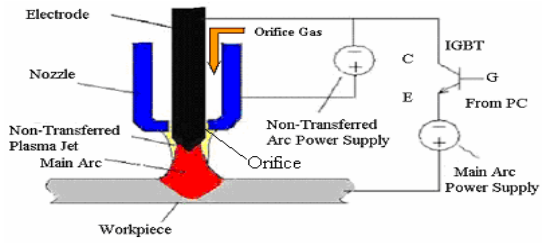

Fig. 2. Integrated GTA Welding/Sensing System

This paper aims at the establishment of an arc sensor based robust control system for gas tungsten arc weld pool surface. To this end, Section 2 proposes an integrated welding/sensing system which uses a non-transferred arc to measure the weld pool surface. The need for an adaptive interval control algorithm is justified and the algorithm is presented in Section 3. Section 4 devotes to the modeling and identification of the dynamic uncertain process to be controlled. In Section 5, the closed-loop control experiments are conducted to verify the effectiveness of the developed system. Finally, conclusions are drawn in Section 6.

2. INTEGRATED SYSTEM

The proposed sensor is based on a non-transferred arc which is typically used in PAW and has the ideal behavior as shown in Fig. 1(b). Fig. 2 proposes the integrated welding and weld pool surface sensing system. In this system, the PAW torch is used but the tungsten electrode extends out of the orifice so that the welding arc is not subject the constraint of the orifice. Although such an arc has been referred to as the soft plasma arc because of the equipment used, it is actually closer to a gas tungsten arc than to a plasma arc and can provide the characteristics of a typical gas tungsten arc. As a result, it can be used to perform gas tungsten arc welding. Further, because the primary role of the non-transferred arc in the integrated system is not to serve as a pilot arc as in PAW to help strike the welding arc but being used for measurement, this paper refers the non-transferred arc as the measurement arc to avoid possible confusions.

In the integrated system, when only the measurement arc exists, the electrical potential V_a between the orifice and the weld pool surface is reversely proportional to the distance l (Lu and Zhang, 2004a):

$$l = A/V_a - B \qquad (1)$$

where A and B are two constants. This sensor has been referred to as a non-transferred plasma charge sensor (NTPCS). Because the non-transferred measurement arc is ignited in the nozzle plenum and blown by the orifice gas out of the plenum, it is not rooted on the weld metal. Hence, the non-transferred measurement arc is straight as ideal shown in Fig. 1(b) and is not subject to possible effect of the weld pool surface geometry. As a result, V_a can accurately reflect the length between the electrode and the weld pool surface. However, this indicative property is destroyed when the main welding arc exists. In order to implement the non-transferred plasma charge sensing mechanism during welding, an isolated gate bipolar transistor (IGBT) power module is utilized to temporarily switch off the main power supply. When the main arc is off, only the measurement arc is present and the sensing can be done automatically. Welding can be carried out any time when needed by switching the main arc on via the IGBT.

Measurement of the weld pool surface requires a flat reference surface (Fig. 3(a)) be established and the surface (Fig. 3(b)) be measured at an appropriate time. First, to obtain a flat reference surface, the main current can be switched off for a sufficient period in

order to allow the weld pool to reduce. As can be seen in Fig. 4, after the main current is switched off, the sensor signal increases and approaches a constant, indicating that the weld pool surface has been flat. Hence, the reference signal should be measured when the sensor signal becomes constant. Second, the weld joint penetration is determined by the maximum weld pool and the weld pool is likely to be the maximum when the main current is switched off. As a result, in this study, the first point (point A in Fig. 4) whose 5 millisecond-average signal is not 0.01V higher than that of the previous one is used as the reference and the average is used as the reference V_a^0 to represent l^0 (Fig. 3(a)); and V_a sampled at the beginning of the sensing period, i.e., point B in Fig. 4, is used to represent the deepest weld pool surface l. The weld pool depth d can thus be expressed as:

$$d = l - l^0 = \frac{A}{V_a} - \frac{A}{V_a^0} = A\frac{V_a^0 - V_a}{V_a V_a^0} = A\frac{\Delta V_a}{V_a^0 V_a}. \quad (2)$$

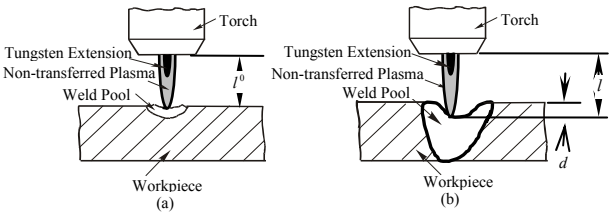

Fig. 3. Monitoring of Weld Pool Surface. (a) Flat Reference Weld Pool; (b) Measured Weld Pool

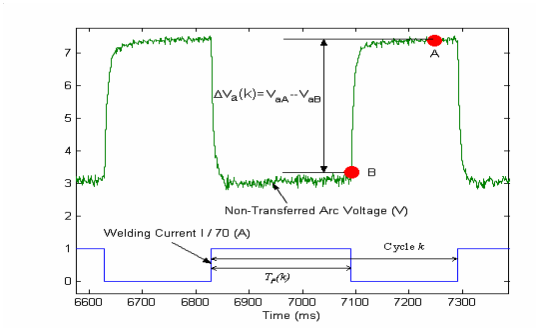

Fig. 4. Typical NTPCS Signal

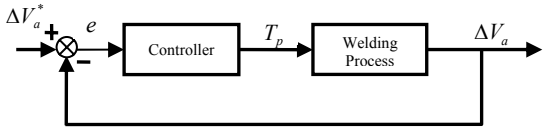

Fig. 5. Illustration of the Control System

where A is a constant as mentioned earlier and $\Delta V_a = V_a^0 - V_a$ is referred to as the relative voltage. As $V_a^0 V_a$ only varies in a small range in comparison with ΔV_a, the weld pool depth d can be considered proportional to ΔV_a. In order to maintain the weld pool surface at a desired level, the relative arc voltage ΔV_a is chosen as the system output y. Because the maximum weld pool is determined by the main-arc-on period T_p when the amperage and travel speed are given, T_p is chosen as the system input u. The process to be controlled can thus be considered as a single-input single-output discrete-time system whose input u_k in cycle k (Fig. 4) is the main-arc-on duration $T_p(k)$ and output y_k is the relative arc voltage $\Delta V_a(k)$ which is the difference between the signals measured at point A and B. The goal of this study is to design a controller (Fig. 5) which adjusts u_k to control y_k at the desired level despite possible variations/changes in the manufacturing conditions.

3. ADAPTIVE INTERVAL MODEL CONTROL

Manufacturing applications demand robust control due to its high disturbance, variation and fluctuation. A number of researches have addressed advanced control of welding process (Zhang and Liu, 2003; Chen *et al*, 2004; Li, 2001). The prediction-based interval model control envelops system uncertainties with parameter maximum and minimum obtained from extreme-condition experiments. Previous studies have shown that it is an effective approach for the control of welding processes where large variations and uncertainties exist (Lu and Zhang *et al*, 2004b). In this study an adaptive interval model control algorithm will be used which can online update model parameters' intervals for quicker response and superior performance.

The original interval model control algorithm (Zhang and Kovacevic, 1997) is based on linear systems described using an impulse response model:

$$y_k = \sum_{j=1}^{n} h(j) u_{k-j} \quad (3)$$

where k is the current instant, y_k is the output at k, u_{k-j} is the input at $(k-j)$ $(j>0)$, while n and $h(j)'s$ are the order and the real parameters of the impulse response function. $h(j)'s\,(1 \le j \le n)$ are unknown but bounded by the intervals:

$$h_{\min}(j) \le h(j) \le h_{\max}(j) \quad (j = 1, ..., n) \quad (4)$$

where $h_{\min}(j) \le h_{\max}(j)$ are the minimum and maximum value of $h(j)$ and known.

Assume the control actions are kept unchanged after instant k, i.e., $\Delta u_{k+j} = 0\,(\forall j > 0)$. Predicting the output n-step-ahead yields:

$$y_{k+n}(\Delta u_k) = y_k + \sum_{j=2}^{n} h(j)(u_{k-1} - u_{k-j}) + s(n)\Delta u_k \quad (5)$$

where $\Delta u_{k-j} = u_{k-j} - u_{k-j-1}$, $s(n)$ is the unit step response whose upper and lower limits have the same polarity. It is apparent

$$y_{k+n}(\Delta u_k) = y_{k+n}(\Delta u_{k-1}) + s(n)\Delta u_k \quad (6)$$

where $y_{k+n}(\Delta u_{k-1}) \overset{\Delta}{=} y_{k+n}(\Delta u_k)\big|_{\Delta u_k = 0}$ and $\Delta u_{k+j} = 0\,(\forall j \ge 0)$. The control action Δu_k is thus determined that:

$$\max y_{k+n}(\Delta u_k) = \max y_{k+n}(\Delta u_{k-1}) + \max(s(n)\Delta u_k) = y_0 \quad (7)$$

It has been proved (Zhang and Kovacevic, 1997) that for the interval plant control problem given by Eqs. (3) and (4), the control described in Eq. (7) will yield:

$$\lim_{k\to+\infty} y_k = y_0 \quad (8)$$

To successfully implement this algorithm, the parameter intervals have to be sufficient such that they bound the parameters in all applications of interest. If the range of applications is wide such that the intervals are large, the system stability specified by (8) will be guaranteed but the response speed may become slow. The accomplishment of adaptive control in updating parameters online inspires the idea of adaptive interval model (Zhang and Walcott, 2004), in which the intervals are determined adaptively online. However, it would be cumbersome if the impulse response model (3) is used for online identification due to the large number of variables. To minimize the amount of identified variables, an auto-regressive model may be used. In particular, if the second-order model $y_k = a_1 y_{k-1} + a_2 y_{k-2} + b_1 u_{k-1}$ with transfer function

$$H(z) = \frac{b_1 z^{-1}}{1 - a_1 z^{-1} - a_2 z^{-2}} = \frac{b_1 z^{-1}}{(1-\alpha_1 z^{-1})(1-\alpha_2 z^{-1})} \quad (9)$$

is sufficient for process modeling, it can be converted into the model (3) with the intervals of poles α_1, α_2 and parameter b_1 known (Zhang and Walcott, 2004). When α_1 and α_2 are real and distinctive as will be in this study, the auto-regressive model (9) is equivalent to the impulse response model (3) with:

$$h(j) = b_1(\alpha_1^{j-1} + \alpha_1^{j-2}\alpha_2 + \alpha_1^{j-3}\alpha_2^2 + \ldots + \alpha_2^{j-1}) \quad (10)$$

where $j = 1,2,\ldots,n$. Because b_1 is independent from α_1 and α_2 and they are all positive for the process to be controlled in this study as will be seen in next section, $h_{\max}(j)$ and $h_{\min}(j)$ can be determined as

$$\begin{cases} h_{\max}(j) = b_{1\max} f(\alpha_{1\max}, \alpha_{2\max}) \\ h_{\min}(j) = b_{1\min} f(\alpha_{1\min}, \alpha_{2\min}) \end{cases} \quad (11)$$

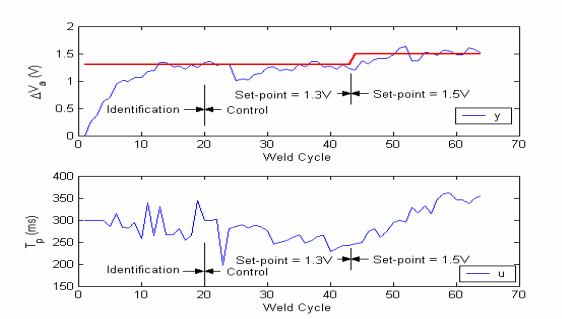

(a) Input/Output

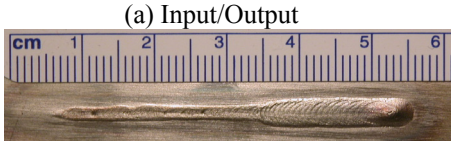

(b) Back-side

Fig. 6. Varied Set-Point Tracking Experiment

where $f(\alpha_1, \alpha_2) = \alpha_1^{j-1} + \alpha_1^{j-2}\alpha_2 + \alpha_1^{j-3}\alpha_2^2 + \ldots + \alpha_2^{j-1}$. Referring to the system (9), the parameters b_1, α_1 and α_2 can be adaptively identified online using the standard recursive least square (RLS) algorithm (Ljung, 1997). In order to find the intervals of the parameters, the parameters obtained in the last n instants are searched and the maximum and minimum are found. Consequently, one can obtain the system model (3) and its parameters' bounds. Following Eq. (5) ~ (7) the interval model control is carried out with the resultant $\{h_{\max}(j), h_{\min}(j)\}$ $(j = 1,2,\ldots)$. It has been pointed out (Zhang and Walcott, 2004) that using poles' intervals inherently guarantees the stability of the interval model and thus provides better intervals for adaptation. From application point of view using the history to determine the stochastic parameter intervals appears advisable and effective.

4. SYSTEM MODELING

As stated earlier, the system input is the main-arc-on duration T_p and the output is the relative arc voltage ΔV_a. Analysis suggests that for the integrated welding/sensing system which periodically switches the main current off, the (maximum) weld pool and pool surface depth achieved should increase as the main-arc-on duration T_p increases. If the main-arc-on duration is not very long, the maximum surface depth achieved should be approximately proportional to the main-arc-on duration. Further, due to the heat accumulation, the pool depth at the k^{th} cycle is not only related to the k^{th} main-arc-on duration, but the previous durations as well. The process to be controlled may thus be modeled as

$$\Delta V_a(k) = h(1)T_p(k-1) + h(2)T_p(k-2) + \cdots + h(N)T_p(k-N) = \sum_{i=1}^{N} h(i)T_p(k-i) \quad (12)$$

where N is the order of the model, $T_p(k-i)$ accounts for the contribution of heat input at the $(k-i)^{th}$ cycle and $\sum_{i=1}^{N} h(i)T_p(k-i)$ denotes the weighted contribution of heat input in the previous N cycles. The units of ΔV_a, $T_p(k-i)$ and $h(i)$'s $(i = 1,2,\ldots,N)$ are volt (V), second (s) and volt/second (V/s), respectively. It is apparent that model (12) is an impulse response model as Eq. (3). Its order N and coefficients $h(i)$'s can be determined experimentally using *F*-test and standard least square method (Astrom and Wittenmark, 1995).

Fig. 2 shows the schematic of the experimental system. The main power supply and measurement arc power sources are two inverters. The IGBT's maximum capacity is rated 300A and 600V. A host computer controls the on/off state of the IGBT and the travel speed of the manipulator which holds the welding torch. All experiments are beads on stainless steel (type 304) plates whose dimensions are $300\,\text{mm} \times 50\,\text{mm} \times 2\,\text{mm}$. Pure Argon gas is used as the orifice gas and shielding gas. The measurement arc

current and the orifice gas flow rate are fixed at 10A and 2.3 L/Min, respectively. The diameter of the orifice is 4.5mm and the tungsten stretches out 1.5mm. The distance between the tungsten tip and work is 4mm. Torch travels at 2mm/s. The Process is sampled at 1KHz.

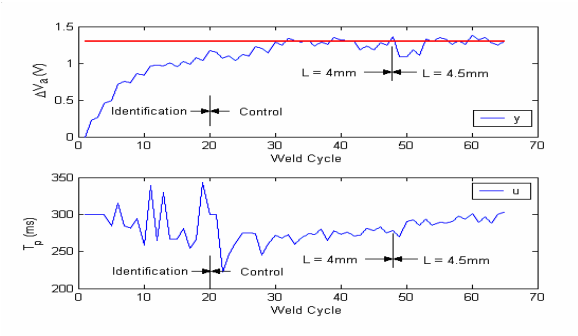

(a) Input/Output

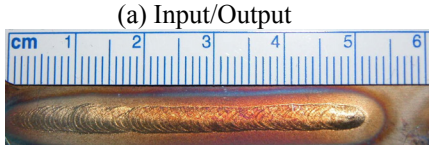

(b) Back-side

Fig. 7. Experiment under Varied L

Before the identification experiments are carried out, some issues must be clarified. First, the main-arc-on current must be determined. For critical joining, full penetration must be guaranteed. To this end, sufficient heat energy must be provided. It is experimentally determined that 70A welding current is adequate to penetrate the plates and the welding current is thus fixed at 70 A. Another issue is how long the sensing period, i.e. the main-arc-off duration, should be. As mentioned earlier, the reference is not taken until the weld pool becomes smooth and flat. It is found that the non-transferred arc sensor signal needs at least 100ms to become relatively steady after the main arc is off. This study uses 200ms to assure the steady state of the weld pool. Third, the welding process is highly stochastic. The weld pool surface might undergo considerable variations even when all process parameters are fixed. This is because the weld pool is not only determined by the deterministic factors, but is the result of balance among all forces which governs the fluid flow, such as pool surface tension, gravity, etc. To reduce the influence of system fluctuation and improve the prediction accuracy, the system output is pre-filtered using a low pass filter with a transfer function:

$$H_f = (1-\beta)/(1-\beta z^{-1}) \qquad (13)$$

which has static gain $(1-\beta)/(1-\beta)=1$. Simulation results show that $\beta = 0.8$ provides good transient response and noise reduction. Fourth, in order to on-line identify the model parameters and conduct adaptive interval model control, the model structure as shown in Eq. (9) has to be used. Denote the transfer function of the plant as $H_p(z)$. The process to be controlled will be:

$$H(z) = H_f(z)H_p(z) = \frac{0.2}{(1-0.8z^{-1})}H_p(z) \qquad (14)$$

To identify the system model, four extreme condition experiments, with the pair (v,L) (where v is the travel speed and L the electrode-to-work distance) to be $(1.25mm/s, 3\text{mm})$, $(2.5mm/s, 3\text{mm})$, $(2.5mm/s, 5\text{mm})$ and $(1.25mm/s, 5\text{mm})$, are conducted. System is persistently excited with random input in the range of [100, 500] milliseconds. Using Least Square (LS) algorithm and F-test on the resultant input-output pairs, it is found that all four sets of experimental data can be modeled as a first-order system, i.e., $H_p(z) = bz^{-1}/(1-\alpha z^{-1})$ and the resultant intervals for (b,α) are $0.0658 < b < 0.6107$ and $0.7721 < \alpha < 0.9813$. As a result, the controlled process can be described as

$$H(z) = H_f(z)H_p(z) = \frac{b_1 z^{-1}}{(1-\alpha_1 z^{-1})(1-\alpha_2 z^{-1})} \qquad (15)$$

with

$$0.013 \le b_1 \le 0.122, 0.772 \le \alpha_1 \le 0.981, 0.8 \le \alpha_2 \le 0.8 \qquad (16)$$

Eq. (11) can then be used to calculate intervals in (4). In the real-time control, the parameters in $H_p(z)$ will be adapted online. The intervals are obtained at each cycle from the maximum and minimum of the identified parameters in the past 20 cycles. If the intervals fall into the *a prior* intervals identified from the extreme experiments as shown in (16), the on-line identified intervals are accepted and used. Otherwise, the accuracy of the on-line identification is questioned and the *a prior* intervals are used.

5. EXPERIMENTAL RESULTS

To test the robustness of the developed system, bead-on-plate welding is conducted. Each experiment is initialized by using random input in the range 200~400 ms for 20 weld cycles. During this period the parameters are identified and their bounds are searched. However, they are not implemented until the closed-loop control begins at the 21st weld cycle.

5.1 Tracking Varied Set Point

In this experiment, the desired output is changed from 1.3V to 1.5V at the 43rd weld cycle. The resultant system output and input are plotted in Figure 6(a) and the corresponding back-side weld is shown in (b). As can be seen, the system reached its first desired output relatively quickly. Once the set point is switched to a higher level, the controller rapidly adjusted the input so that the input increased from 270ms to about 350ms. As a result, the weld pool surface depth increased to its new desired level.

5.2 Electrode-to-work Distance Variation Experiment

During welding, the electrode-to-work distance may vary. To assure the sensor's robustness and accuracy, this paper proposes periodically establishing the reference surface. To test the effectiveness of the proposed method, in this experiment, the electrode-to-work distance L changed from 4 mm to 4.5mm at the 48th cycle. Figure 7 (a) shows the resultant input/output and (b) shows the back-side of the weld.

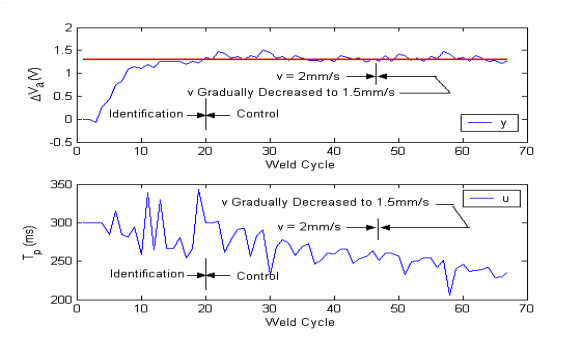

(a) Input/Output

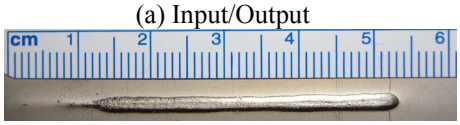

(b) Back-side

Fig. 8. Experiment under Varied v

It is evident that system output was first stabilized at the set point quickly after the closed-loop control is applied. When the distance increased, the conically shaped gas tungsten arc resulted in a larger arc contacting zone on the weld pool and the arc pressure decreased. Thus, the output, i.e., the weld pool surface depth, decreased. As can be seen in Figure 7(a), the input increased quickly to compensate it.

5.3 Speed Variation Experiment

Travel speed is a critical parameter in welding process. In this experiment, the travel speed v was 2mm/s in the first 47 cycles. From the 48th cycle, the manipulator that carries the torch was modulated so that the travel speed gradually decreased from 2mm/s to 1.5mm/s. Figure 8(a) shows the experimental input and output. The back-side of the weld is shown in (b). It is apparent that, due to the closed-loop control, the input has been adjusted to maintain output around the desired level despite the variation in the travels peed.

6. CONCLUSION

The integrated welding/sensing system proposed provides a method to conduct the precision gas tungsten arc welding with a controlled weld pool surface. Because of the durable non-transferred plasma charge sensor, the proposed system appears suitable for welding applications under manufacturing environment. The use of the on-line reference surface tracking improves the robustness and adaptability of the proposed system.

Interval model provides an effective way to model uncertain welding process. However, fixed intervals, while guaranteeing the stability, may reduce the response speed. The adaptive interval model control, which uses the online updated intervals to achieve speed and uses *a prior* intervals to guarantee the stability, appears a sound solution. Experimental results under varied manufacturing conditions verified the effectiveness of the developed sensing/control system for weld pool surface depth during gas tungsten arc welding.

ACKNOWLEDGEMENTS

This work is funded by NSF under Grant DMI-0114982. Supplemental funding is provided by the Magnatech Limited Partnership, East Granby, Connecticut, and NSF GOALI Program.

REFERENCES

American Welding Society (1990). *Welding Handbook* **Vol. 2**: *Welding Processes*. 8th edition.

Anedenroomer, A.J.R. and den Ouden, G. (1998). Weld pool oscillation as a tool for penetration sensing during pulsed GTA welding. *Welding Journal*, **77(5)**, pp. 181s-187s.

Astrom, K.J, and Wittenmark, B. (1995). *Adaptive Control*, 2nd edition. Addison-Wesley.

Bai, M., Ume, I.C. (2004). Three-dimensional ray tracing of laser ultrasound for weld penetration sensing. *Journal of the Acoustical Society of America*, **115 (4)**: 1565-1571.

Chen, Q., Sun, Z.G., Sun, J.W., Wang, Y.W. (2004). Closed-loop control of weld penetration in keyhole plasma arc welding. *Transactions of Nonferrous Metals Society of China*, **14 (1):** 116-120.

Chen, S.B., Lou, Y.J., Wu, L., Zhao, D.B. (2000). Intelligent methodology for sensing, modeling and control of pulsed GTAW: Part I - Bead-on-plate welding. *Welding Journal*, **79 (6):** 151s-163s.

Chen, S.B., Zhao, D.B., Lou, Y.J., Wu, L. (2004). Computer vision sensing and intelligent control of welding pool dynamics. *Robotic Welding, Intelligence and Automation Lecture Notes in Control and Information Sciences*. **299:** 25-55 2004.

Fan, H., Ravala, N.K., Wikle, H.C, Chin, B.A. (2003). Low-cost infrared sensing system for monitoring the welding process in the presence of plate inclination angle. *Journal of Materials Processing Technology*, **140:** 668-675.

Gao, J., Wu, C. (2003). Neurofuzzy control of weld penetration in gas tungsten arc welding. *Science and Technology of Welding And Joining*, **8 (2):** 143-148.

Hopko, S. N. and Ume, I. C. (1999). Laser generated ultrasound by material ablation using fiber optic delivery. *Ultrasonics*, **(37)1:** pp. 1-7.

Koseeyaorn, P., Cook, G. E. and Strauss, A. M. (1999). Adaptive voltage control in fusion arc welding. *IEEE Industrial Applications Society the Thirty-fourth Meeting*, Session 55, Power Electronics Components and Devices, pp 2393-2395.

Li, X.C., Farson, D., Richardson, R. (2001). Weld penetration control system design and testing. *Journal of Manufacturing Systems,* **19 (6):** 383-392.

Ljung, L. (1997). *System Identification—theory for the user,* 2nd edition Prentice-Hall, Upper Saddle River, NJ.

Lu, W., Zhang, Y. M. and Emmerson, J. (2004a). Sensing of weld pool surface using non-transferred plasma charge sensor. *Measurement Science and Technology*, **15:** 991–999.

Lu, W., Zhang, Y. M., and Lin, W-Y. (2004b). Nonlinear interval model control of quasi-keyhole arc welding process. *Automatica,* **40:** 805 – 813.

Renwick, R. J. and Richardson, R. W. (1983). Experimental investigation of GTA weld pool oscillations, *Welding Journal*, **62(2)**: 29s-35s.

Zhang, C. and Walcott, B. L. (2004). "Adaptive interval model control and application," *Proceedings of the 2004 American Control Conference*, June 30-July 2, Boston, MA.

Zhang, Y.M. (1990). *Front-side Vision Based Adaptive Control of Weld Joint Penetration*. PhD Dissertation, Harbin Institute of Technology, Harbin, China.

Zhang, Y. M., and Kovacevic, R. (1997). Robust control of interval plants: A time domain approach. *IEE Proceedings-Control Theory and Applications*, **144(4),** 347-353.

Zhang, Y.M. and Liu, Y.C. (2003). Modeling and control of quasi-keyhole arc welding process. *Control Engineering Practice*, **Vol. 11:** 1401-1411.